Exp Biomed Res 2026; 9(4): 348–366 https://doi.org/ 10.30714/j-ebr.2026.292

Experimental Biomedical Research *Original article*

# Mandibular measurements derived from computed tomography for sex estimation in a geriatric Turkish population: A machine learning approach

**Mahmut Kurtboğan[1], Gülçin Ray[2], Abdullah Ray*[2]**

[1]*Department of Orthopedics and Traumatology, Faculty of Medicine, Bolu Abant İzzet Baysal University, Bolu, Türkiye*

[2]*Department of Anatomy, Faculty of Medicine, Bolu Abant İzzet Baysal University, Bolu, Türkiye*

## ABSTRACT

**Aim:** To assess the rate of sexual dimorphism in a healthy, geriatric Turkish population through the evaluation of selected mandibular variables on computed tomography (CT) scans where the cranium is displayed in three dimensions via machine learning algorithms (MLA).

**Methods:** The study sample consisted of 120 females and 120 males aged 65 or above. Fourteen linear mandibular variables were measured on three-dimensional CT images of the cranium, including right and left maximum ramus height (RMXRH, LMXRH) and bi-gonial breadth (BGP). The machine learning algorithms utilised in the study are as follows; Random Forest (RandForest), Logistic Regression (LogReg), Linear Discriminant Analysis (LDA), Gradient Boosting (GradBoost), Support Vector Machine with Radial Basis Function Kernel (SVM (RBF)), Support Vector Machine with Linear Kernel (SVM (Linear)), and K-Nearest Neighbors (KNN), Decision Tree (DecTree), Naive Bayes, and AdaBoost.

**Results:** Statistically significant differences between sexes were found for all variables. The highest accuracy rate for MLA was obtained via Random Forest algorithm (Acc = 0.938). The LogReg, LDA, GradBoost, SVM (RBF), SVM (Linear), and KNN algorithms achieved the same accuracy rate (Acc = 0.917). The highest AUC values were observed in the LogReg and LDA algorithms based on the calculated ROC curve, with both models achieving an identical AUC score (AUC = 0.979). It was found that the most significant variable in sex prediction was RMXRH (importance score = 0.1686), followed by LMXRH (0.1234) and BGP (0.0908).

**Conclusion:** It was found that the selected linear mandibular variables present high accuracy rates in determining the sex of geriatric Turkish population via MLA.

**Keywords:** Mandibular morphometry, sex estimation, CT scan images, machine learning algorithms, forensic anthropology.

*Corresponding author: Abdullah Ray*
*Department of Anatomy, Faculty of Medicine, Bolu Abant İzzet Baysal University, Bolu, Türkiye*
*E-Mail: abdullahray10@gmail.com*

*Received: 2026-08-09 / Revisions: 2026-09-11*
*Accepted: 2026-09-16 / Published: 2026-10-01*

## 1. Introduction

Forensic anthropology aims to identify human remains whose integrity is compromised because of natural disasters such as earthquakes and fires, wars and large-scale catastrophes, and investigates age, sex, height and race as criteria [1,2]. The first step of anthropological investigations includes determining the sex as establishing the sex provides a reference for the other criteria [1]. While DNA analysis is proven to be the most reliable method, it is not largely favoured due to its cost and time restrictions. At this stage, a sub-branch of artificial intelligence, MLA emerges as a highly accurate method with minimal labour and cost [3].

The recent strides in forensic health sciences include identification effort where both anthropometric datasets and MLA are utilised.

As the bone tissue retains its structural integrity in post-mortem settings, bones are frequently subjected to forensic health science studies [4]. Pelvis and cranium are widely regarded as the bones which reflect sexual dimorphism the best [1,4,5]. However, in cases where the complete pelvis and cranium cannot be accessed, the forensic anthropologists employ fragments of these bones or other bones for sex determination [6].

The mandible, the subject of this study, is both the largest and the strongest bone in the facial skeleton and is more durable against environmental factors than other facial bones due to its more compact structure [5,6]. The mandible, the only mobile bone of the cranium, consists of two parts: the corpus and the ramus. It articulates solely with the temporal bone and is the first structure to commence ossification after the clavicle. The foramina through which important anatomical structures pass, together with the key anatomical landmarks where the masticatory muscles attach, were employed as reference points in the present study [7,8]. Throughout the post-natal period, it also grows faster and changes shape more rapidly when compared to the other facial bones [9].

Studies on this subject show that the mandible displays sexual dimorphism starting from the utero; and that its characteristics become more pronounced during puberty [9-11]. When the studies in the literature where bone collections [12,13] and CT [5-9] images are employed to determine the mandibular variables, it is seen that the mandible clearly reflects sex-related differences starting from the pediatric period [9,11]. Also, to the best of researchers' knowledge, no studies on determining sex via the mandible in the geriatric population has been identified in the literature. The CT technology which allows for clear imaging and evaluation of skeletal structures has recently become preferred in sex determination studies [9]. As the accuracy ratings obtained in these studies are population-specific, it is also observed that each population concluded different findings [1,5,6,11]. This indicates that the sexual dimorphism rates therefore require to be population specific [11]. In light of the information provided, the study was designed to evaluate the viability of data derived from mandibular variables to determine sex in the geriatric Turkish populations through examining sex-specific differences, and to compare these findings with the relevant literature.

## 2. Materials and methods

The study was designed as retrospective and cross-sectional and was conducted between October 2025 and March 2026. Ethical approval for this study was obtained from the BAIBU Clinical Research Ethics Committee under decision number 2026/09. As the study data was obtained through randomly selected images in BAIBU PACS archive, no informed consent form was signed. The study sample consists of 240 individuals aged 65 and older (120 females, 120 males). CT imaging was carried out with a 64-detector row scanner (Revolution EVO, GE Healthcare, Waukesha, WI, USA). A standard-dose acquisition protocol was employed, operating at a tube voltage of 120 kVp with automatic tube current modulation. The images in which the entire mandible could not be seen, those belonging to younger than 65 years of age, those showing pathological conditions affecting the shape and size of the mandible and those with poor clarity of image were excluded from the study. Between December 2025 and February 2026, images with a slice thickness of 0.625 mm were converted to DICOM format, imported into the Radiant DICOM Viewer (RDV) software, and converted to 3D MPR. A total of 14 variables

were measured in the study; bi-condylar breadth (BCB), bi-mental foramina breadth (BMFB), bi-antegonial notch breadth (BANB), bi-gonial breadth (BGP), right maximum ramus height (RMXRH), right maximum mandibular body length (RMMBL), right maximum ramus breadth (RMXRB), right minimum ramus breadth (RMNRB), right maximum mandibular length (RMML), left maximum ramus height (LMXRH), left maximum mandibular body length (LMMBL), left maximum ramus breadth (LMXRB), left minimum ramus breadth (LMNRB) and left maximum mandibular length (LMML). For the BCB variable, the distance between the terminal points of the condyles; for BGP variable, the distance between the gonion points on both sides; for BANB variable, the distance between the antegonial notches on both sides; and for the BMFB variable, the distance between the mental foramina on both sides were measured.

Additionally, in lateral views, the distance between the mental tubercle and the posterosuperior aspect of the mandibular condyle is used as the MML variable for the right and left sides.

The distance between the mental tubercle and the gonion is used as the

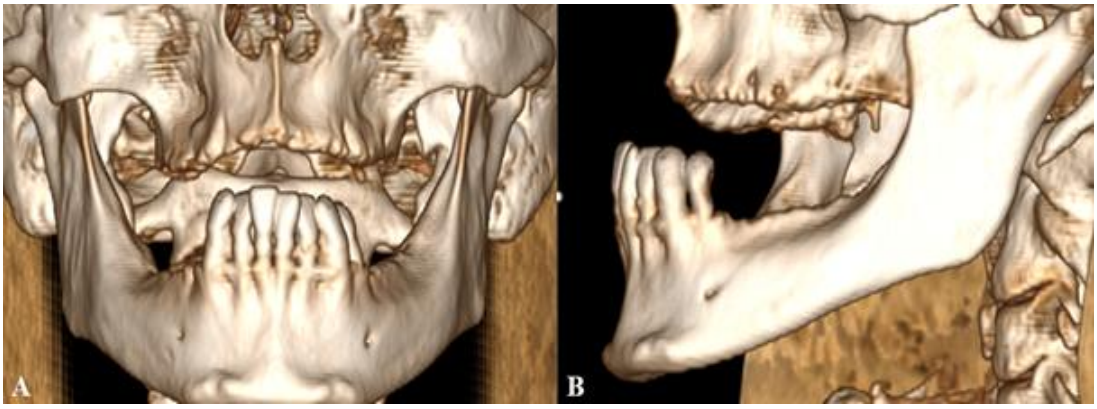


**Figure 1.** 3D MPR CT image of the cranium of an 85-year-old male participant (A. anterior view, B. left lateral view).

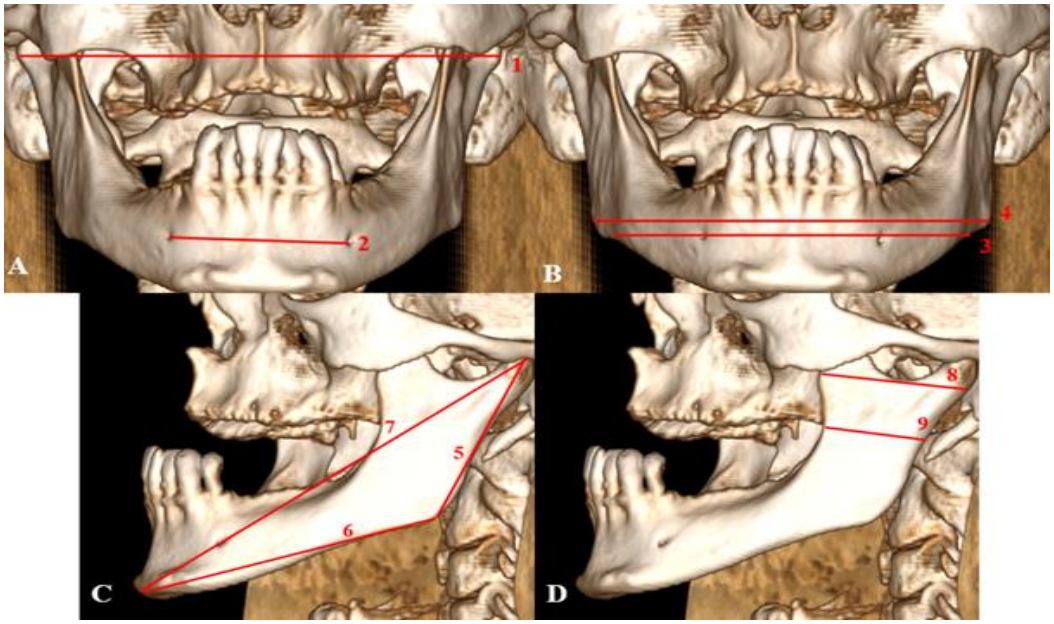


**Figure 2.** Mandibular parameters used for sex determination and their corresponding location on 3D MPR image. **A.** 1- bi-condylar breadth (BCB), 2- bi-mental foramina breadth (BMFB). **B.** 3- bi-antegonial notch breadth (BANB), 4- bi-gonial breadth (BGP). **C.** 5- left maximum ramus height (LMXRH), 6- left maximum mandibular body length (LMMBL), 7- left maximum mandibular length (LMML). **D.** 8- left maximum ramus breadth (LMXRB), 9- left minimum ramus breadth (LMNRB).

MMBL variable; and the distance between the highest point of the mandibular condyle and the gonion is used as the MXRH variable; and in the MXRB variable, the distance between the lowest point of the mandibular condyle and the proccessus coronoideus have been defined as reference points. The measurements were made on anterior and lateral CT cranium images (Figure 1) and measured variables were presented in Figure 2.

***2.1. Statistical Analysis:*** Statistical analyses were made with RStudio. A one-way analysis of variance was conducted for all variables. Then, Anderson-Darling test was applied to assess the normality of residual values from the analysis of variance. Logarithmic and square-root transformations were applied to the nonparametric variables. Normal distribution was observed in the results of the square root transformations of the RMML and LMXRH variables.

To differentiate sex differences on parametric variables, an independent T-test was used. For nonparametric variables, the Mann-Whitney U test was used. The mean, standard deviation, and 95% confidence intervals were calculated for parametric variables; for nonparametric variables, the median, minimum, maximum, and 95% confidence intervals were calculated.

To determine the relationship between parametric variables, the Pearson correlation test was used; while the Spearmen correlation test was employed for nonparametric variables. Logistic regression was then performed, and the ROC curve was plotted to calculate the area under the curve (AUC) and cutoff, sensitivity, and specificity values.

***2.2. Machine Learning Algorithms (MLA):*** The machine learning algorithms were coded in python via Spyder IDE. The machine learning algorithms utilised in the study are as follows; Random Forest (RandForest), Logistic Regression (LogReg), Linear Discriminant Analysis (LDA), Gradient Boosting (GradBoost), Support Vector Machine with Radial Basis Function Kernel (SVM (RBF)), Support Vector Machine with Linear Kernel (SVM (Linear)), and K-Nearest Neighbors (KNN), Decision Tree (DecTree), Naive Bayes, and AdaBoost. The dataset has been split into a training-test ratio of 80%-20%, and 10-fold cross-validation was applied to the dataset. As evaluation metric, a confusion matrix (Cm) table was created and Accuracy (Acc), 10-fold CV accuracy (CV_Acc), ROC-AUC, F1 score, Precision and Recall values were calculated.

## 3. Results

***3.1. Comparative Evaluation of Model Performance***

Ten different MLA models were tested on a binary classification task (F/M) to evaluate classification performance, and a confusion matrix (CM) was created for each model. The highest accuracy rate was achieved with Random Forest algorithm (Acc = 0.938). In this model, all 24 samples in the F class were correctly classified; and only 3 samples from the M class were misclassified, no false negatives were produced (TP_F = 21, FP_F = 0, TP_M = 24, FN_M = 0). The LogReg, LDA, GradBoost, SVM (RBF), SVM (Linear), and KNN algorithms achieved the same accuracy rate (Acc = 0.917) and a similar classification pattern was observed. For the F class, 21 true positives and 3 false negatives were achieved in the LogReg, LDA, GradBoost, and SVM (Linear) models; for the M class, 23 true positives and 1 false negative were achieved. In the SVM (RBF) and KNN models, 22 true positives and 2 false negatives were achieved in F Class, and 22 true positives and 2 false negatives were achieved in M Class. While the DecTree and Naive Bayes algorithms displayed

an equal accuracy rating (Acc = 0.896), they demonstrated moderate performance among the models tested. Both models produced 21 positives and 3 negatives in F class; while DecTree algorithm produced 22 positives and 2 negatives and Naive Bayes produced 22 positives and 2 negatives in M class. The lowest accuracy rate was observed in AdaBoost algorithm (Acc = 0.875). The model produced 21 true positives, and 3 false negatives were obtained for F class and displayed a symmetrical error distribution within both classes. When all models are compared, it was observed that the Random Forest algorithm achieved the highest classification accuracy and produced no false negatives for the M class. Upon an examination of distribution of errors across classes, it was noted that in general, the tendency for samples belonging to M class to be misclassified as F remained at a lower level compared to the misclassification of F class as M. This finding indicates that the models exhibit relatively stronger specificity performance for F Class (Figure 3).

MLA classification performance was comparatively evaluated based on four key metrics (Acc, F1 score, ROC-AUC, and CV_Acc). In terms of test accuracy, the highest performance was achieved by the Random Forest algorithm (0.9375), followed by equal accuracy rates achieved by KNN, SVM (Linear), SVM (RBF), GradBoost, LDA, and LogReg algorithms (0.9170). While Naive Bayes and DecTree performed at a moderate level (0.8958), AdaBoost stood out as the algorithm with the lowest test accuracy (0.8750). The overall average of the models remained at approximately 0.905. In terms of F1 score, Random Forest achieved the highest rating (0.9412). The SVM (Linear), GradBoost, LDA, and LogReg algorithms achieved the same F1 score (0.9200), while KNN and SVM (RBF) scored 0.9167. Naive Bayes and DecTree performed at a moderate level with similar F1 scores (0.8980), while AdaBoost again achieved the lowest rate (0.8750). When ROC-AUC values are examined, it is seen that LDA and LogReg algorithms display the highest discriminative performance (0.9792). These algorithms were followed, in order, by Random Forest (0.9748), SVM (Linear) (0.9740), AdaBoost and GradBoost (0.9722),

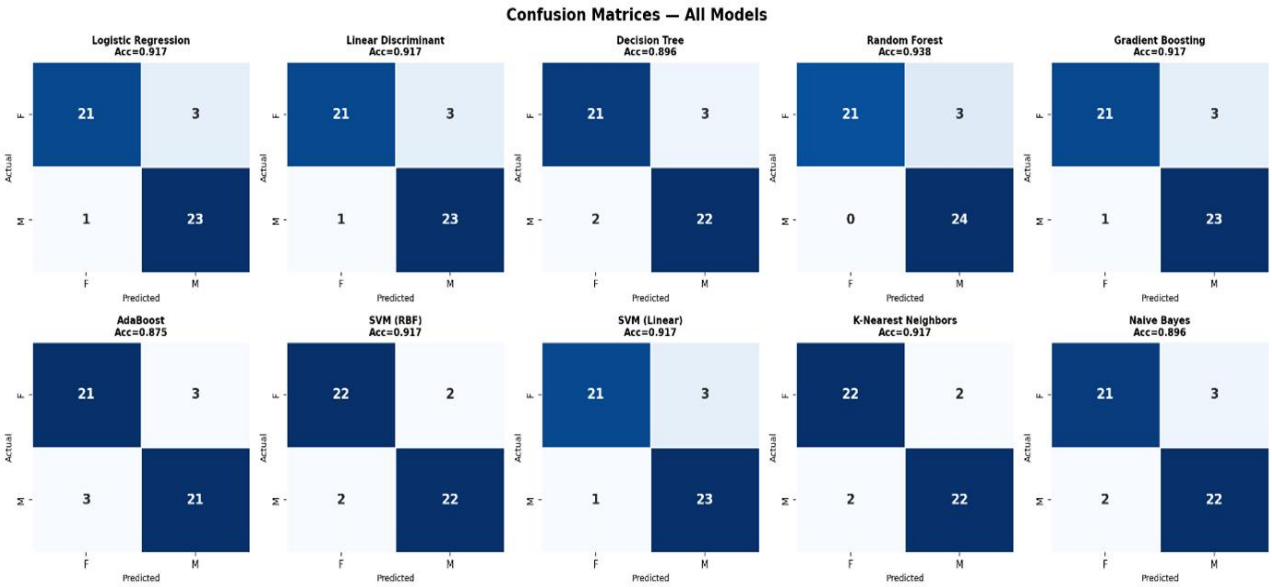


**Figure 3.** Confusion matrix tables showing the performance of algorithms (Random Forest (RandForest), Logistic regression (LogReg), Linear discriminant analysis (LDA), Gradient Boosting (GradBoost), Support Vector Machine with Radial Basis Function Kernel (SVM (RBF)), Support Vector Machine with Linear Kernel (SVM (Linear)) ve K-Nearest Neighbors (KNN), Decision Tree (DecTree), Naive Bayes, AdaBoost).

SVM (RBF) (0.9618), and KNN (0.9670). While Naive Bayes demonstrated a median ROC-AUC value (0.9531), DecTree displayed the lowest discriminative performance among all models (0.8958). An evaluation of cross-validation results show that the AdaBoost algorithm achieved the highest CV accuracy (0.8129); followed, in order, by SVM (Linear) (0.7916), KNN (0.7768), LogReg (0.7711), and Random Forest (0.7668). Naive Bayes (0.7511), LDA (0.7403), and GradBoost (0.7397) demonstrated moderate cross-validation performance. SVM (RBF) (0.7350) and DecTree (0.7247) stood out as the algorithms with the lowest cross-validation accuracy. Graphs showing the algorithms' Acc, F1 score, ROC-AUC, and CV_Acc values are presented in Figures 4 and 5.

ROC curves were calculated for all algorithms, and the area under the curve (AUC) values were analyzed comparatively to evaluate the models' discriminative performance in the binary classification task. All models performed significantly better than the reference line (AUC = 50) corresponding to the random estimate. The highest AUC values were observed in LogReg and LDA algorithms with both models recording an equal AUC score (AUC = 0.979). ROC curves of these models followed the area closest to the top-left corner, effectively achieving a balance between high sensitivity and high specificity. These algorithms were followed by RandForest (AUC = 0.975), SVM (Linear) (AUC = 0.974) and GradBoost & AdaBoost (AUC = 0.972). KNN algorithm displayed a moderate to high discriminative capacity (AUC = 0.967). While SVM (RBF) fell at the lower end of the group (AUC = 0.962), the Naive Bayes algorithm showed acceptable performance (AUC = 0.953). DecTree algorithm stood out as the algorithm with the lowest AUC values across all models (AUC = 0.896). The fact that the ROC curve exhibits a stepped and irregular structure suggests that the model takes decisions based on fixed threshold values rather than generating probability estimates, hence cannot form a continuous curve (Figure 6).

To evaluate the models' generalization performance and cross-validation consistency, 10-fold cross-validation was applied; the resulting accuracy distributions were then visualized using box plots. AdaBoost algorithm achieved the highest median value of approximately 0.81 in terms of median CV accuracy, followed by the SVM (Linear) and KNN algorithms which achieved a median value of approximately 0.79. LogReg and RandForest presented with approximately 0.76 median value, which is regarded as moderate-high median performance. While GradBoost remained at the lower end of this group with a median value of approximately 0.75, SVM (RBF) also performed at a similar level (≈ 0.74). The lowest median CV_Acc values were observed in LDA, DecTree and Naive Bayes algorithms. The median value of all three models was approximately 0.69-0.70. An examination of the interquartile range (IQR) revealed that GradBoost algorithm produces the model with the narrowest distribution and demonstrates high consistency across folds. AdaBoost and SVM (Linear) algorithms demonstrated a consistent performance with their relatively narrow IQR values. However, RandForest stood out as the model with the widest interquantile variance; which suggests that the algorithm demonstrates significant performance fluctuations across different quarters. Naive Bayes, on the other hand, exhibited the most variable performance profile, characterized by both a low median value and a wide interquartile variance. When evaluated in terms of outlier analysis, upward-

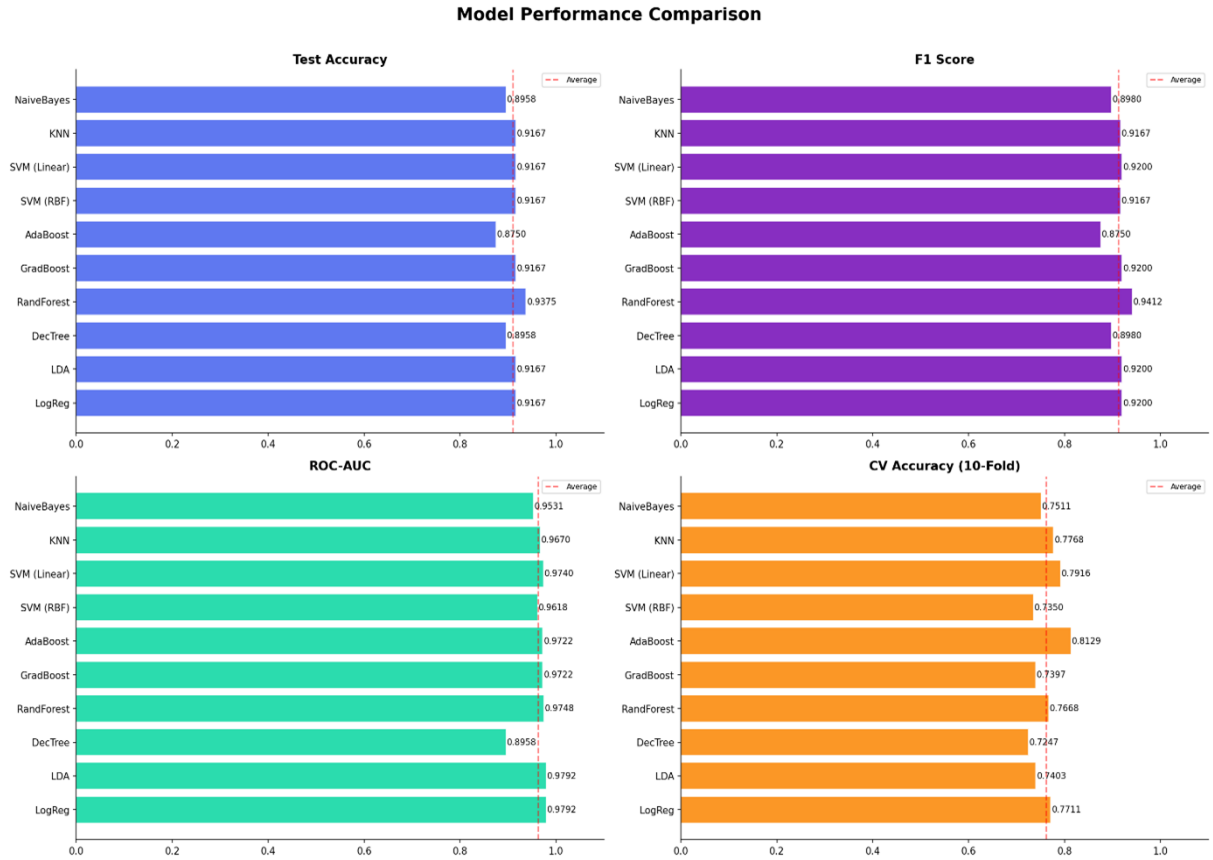


**Figure 4.** Box plots showing the test accuracy (Acc), F1 score, ROC-AUC value, and 10-fold cross-validation accuracy of the algorithms (Random Forest (RandForest), Logistic regression (LogReg), Linear discriminant analysis (LDA), Gradient Boosting (GradBoost), Support Vector Machine with Radial Basis Function Kernel (SVM (RBF)), Support Vector Machine with Linear kernel (SVM (Linear)) and K-Nearest Neighbors (KNN), Decision Tree (DecTree), Naive Bayes, AdaBoost).

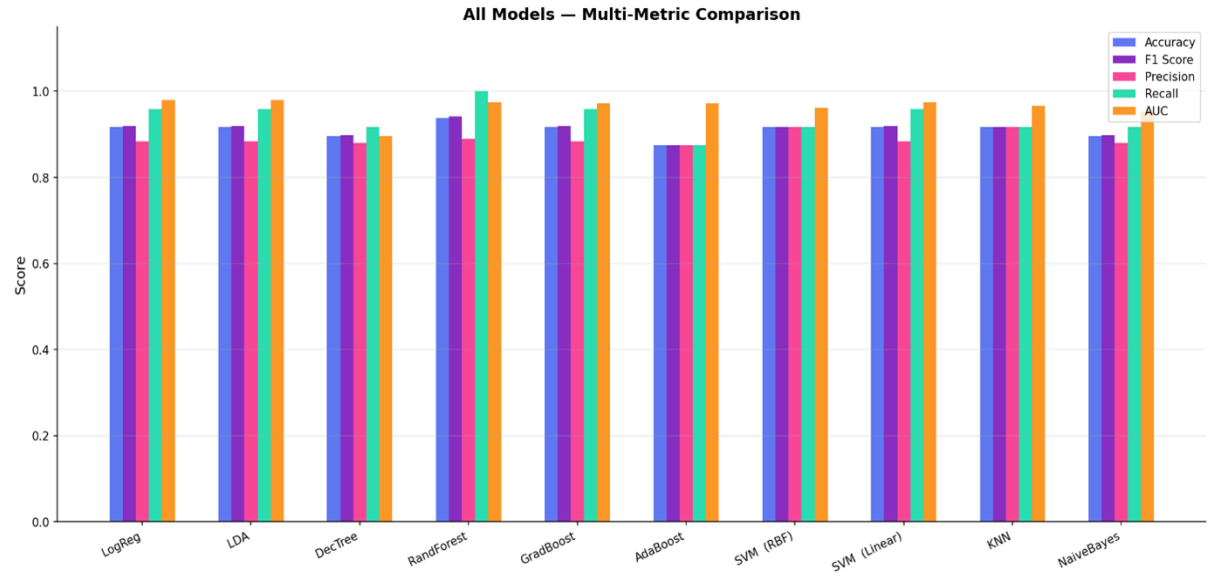


**Figure 5.** Comparison on accuracy, F1 score, ROC-AUC values and Precision and Recall values across algorithms (Random Forest (RandForest), Logistic regression (LogReg), Linear discriminant analysis (LDA), Gradient Boosting (GradBoost), Support Vector Machine with Radial Basis Function Kernel (SVM (RBF)), Support Vector Machine with Linear Kernel (SVM (Linear)) and K-Nearest Neighbors (KNN), Decision Tree (DecTree), Naive Bayes, AdaBoost).

biased outliers were found at approximately 0.95 in the DecTree model and at approximately 1.00 in the AdaBoost model. A downward outlier at approximately 0.58 stood out in the GradBoost algorithm. The presence of these outliers demonstrates that these models may exhibit inconsistent classification performance based on data distribution in specific levels (Figure 7).

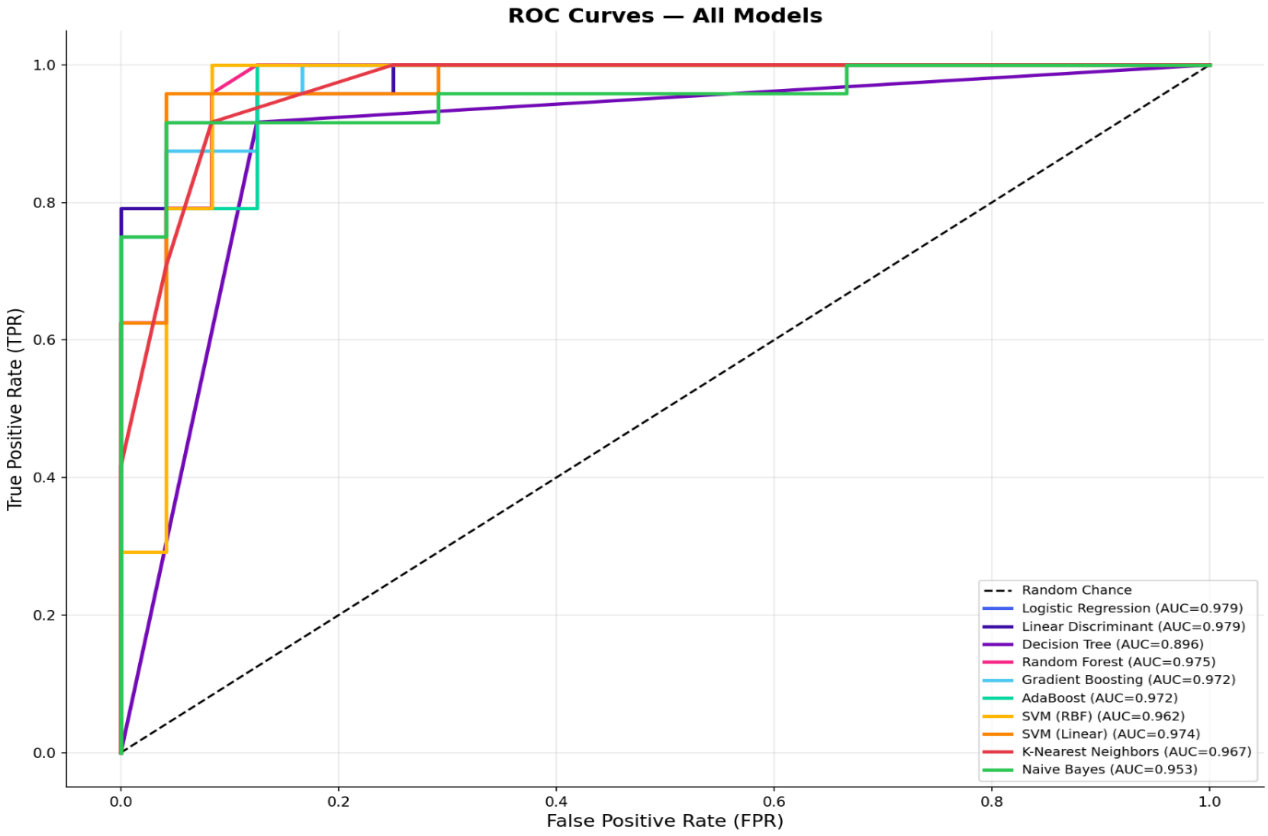


**Figure 6.** ROC curves and AUC values of model performances

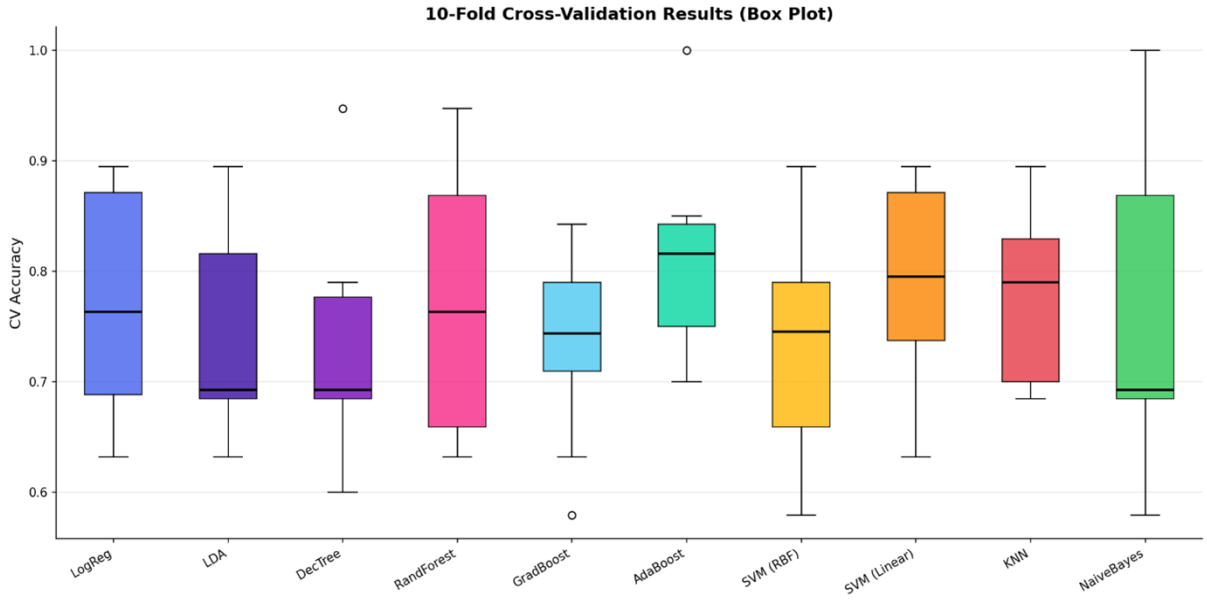


**Figure 7.** Boxplot showing a comparison of cross-validation results across different algorithms (Random Forest (RandForest), Logistic regression (LogReg), Linear discriminant analysis (LDA), Gradient Boosting (GradBoost), Support Vector Machine with Radial Basis Function Kernel (SVM (RBF)), Support Vector Machine with Linear Kernel (SVM (Linear)) ve K-Nearest Neighbors (KNN), Decision Tree (DecTree), Naive Bayes, AdaBoost).

In order to identify which variables play a decisive role in sex prediction, a variable feature importance analysis was conducted based on the RandForest algorithm. The results are presented in Figure 8. According to the analyses, RMXRH appears to be the most significant variable in sex prediction (importance score = 0.1686). This variable is followed by LMXRH (0.1234) and BGP (0.0908), respectively. These three variables account for approximately 30% of the total variable importance score and therefore play a dominant role in the model's classification decisions. It is also notable that the LMML (0.0854), RMML (0.0836), BCB (0.0775), and BMFB (0.0696) variables cluster together with similar importance scores at the moderate level. These variables provide significant but secondary contributions to the predictive strength of the algorithm. Among the variables that contributed relatively less are LMMBL (0.0493), LMXRB (0.0466), LMNRB (0.0446), RMMBL (0.0429), and BANB (0.0429). The lowest importance scores were observed in RMXRB (0.0390) and RMNRB (0.0359) variables.

The mean age of the individuals included in the study was 73 (65–99), with a 95% confidence interval of 71–77. The median, minimum, and maximum values were 76 (65–96) (95% CI: 73–80) for males and 75 (60–99) (95% CI: 73–77) for females; no statistically significant difference was found between the sexes (P = .118). The mean and standard deviation values of the measured variables, along with their confidence intervals, were as follows for males and females, respectively: BCB 12.5±0.5 (95% CI: 12.4–12.6) and [female BCB value to be inserted: mean±SD (95% CI)], BANB 9.3±0.6 (95% CI: 9.2–9.4) and 8.8±0.5 (95% CI: 8.7–8.9), BGP 10.3±0.6 (95% CI: 10.2–10.4) and 9.6±0.6 (95% CI: 9.5–9.7), RMXRH 6.1±0.5 (95% CI: 6.0–6.2) and 5.4±0.5 (95% CI: 5.3–5.5), LMMBL 8.8±0.6 (95% CI: 8.7–8.9) and 8.3±0.5 (95% CI: 8.2–8.4), LMXRB 3.8±0.4 (95% CI: 3.7–3.9) and 3.5±0.4 (95% CI: 3.4–3.6), LMNRB 2.8±0.3 (95% CI: 2.8–2.9) and 2.6±0.3 (95% CI: 2.6–2.7), RMML 3.5±0.1 (95% CI: 3.5–3.5) and 3.4±0.1 (95% CI: 3.3–3.4), LMXRH 2.4±0.1 (95% CI: 2.4–2.4) and 2.2±0.1 (95% CI: 2.2–2.3). For variables that do not follow a normal distribution, the median, minimum, and maximum values were identified as follows for males and females, respectively: BMFB 4.3 (0.5–5.0) (95% CI: 4.2–4.4) and 4.4 (0.5–6.1) (95% CI: 4.3–4.5), RMMBL 8.0 (5.2–9.4) (95% CI: 7.9–8.1) and 8.2 (5.2–10.5) (95% CI: 8.0–8.3), RMXRB 4.0 (2.6–5.07) (95% CI: 3.8–4.0) and 4.1 (2.6–5.2) (95% CI: 4.0–4.1), RMNRB 2.9 (1.9–4.1) (95% CI: 2.8–3.0) and 3.0 (1.9–4.2) (95% CI: 2.9–3.0), LMML 11.7 (8.3–14.0) (95% CI: 11.6–11.9) and 12.1 (8.3–15.0) (95% CI: 11.9–12.2). It was concluded that sex differences were significant for all variables. The descriptive statistics for the variables and the results of the tests conducted to assess differences between sexes are presented in Table 1.

A Pearson correlation analysis was conducted to evaluate the relationships among variables that follow a normal distribution, and the results are presented in Figure 9. When findings are examined, a strong and positive correlation was found between BANB and BGP variables (r = .76). Similarly, a high positive correlation was observed among the LMXRB and LMNRB variables (r = .79). The correlation between RMXRH and LMXRH was found to be remarkably strong (r = .75), hinting that these two variables show a significant degree of overlap. It can also be noted that the correlation coefficients between all pairs of variables are positive and range from .16 to .79. No negative

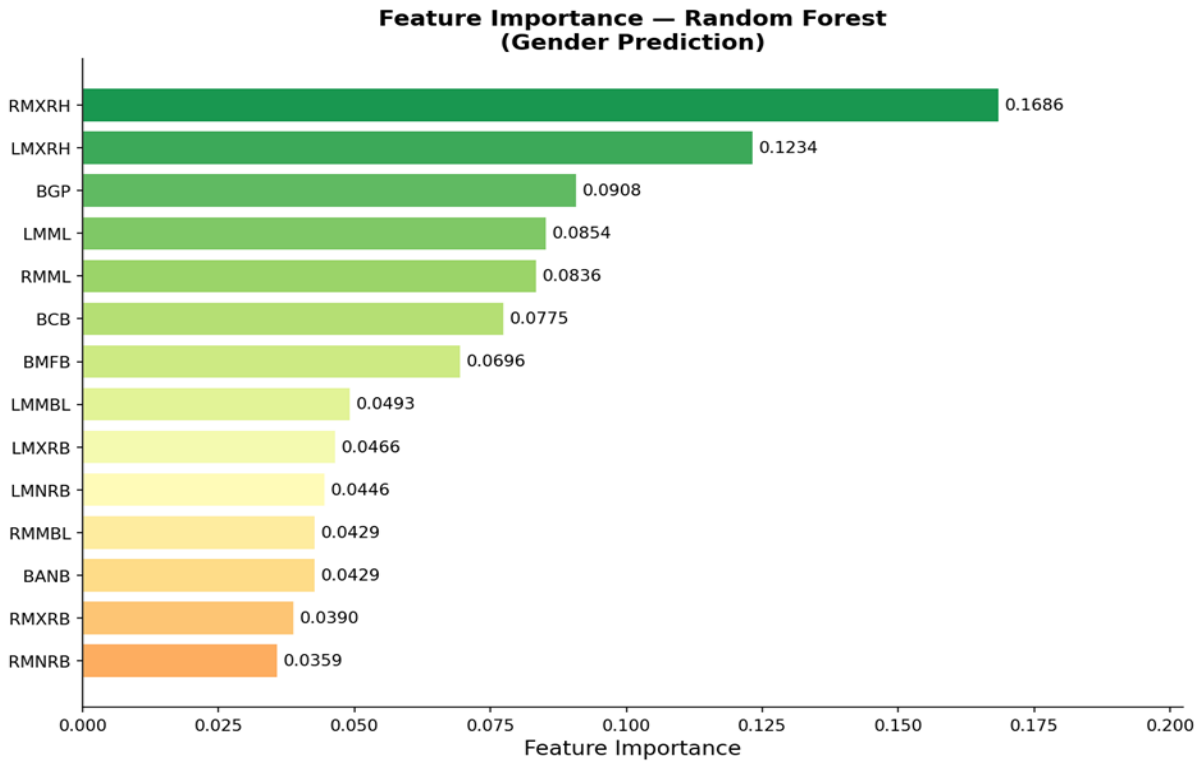


**Figure 8.** Box plot showing variable importance analysis (BCB: bi-condylar breadth, BMFB: bi-mental foramina breadth, BANB: bi-antegonial notch breadth, BGP: bi-gonial breadth, LMXRH: left maximum ramus height, LMMBL: left maximum mandibular body length, LMML: left maximum mandibular length, LMXRB: left maximum ramus breadth, LMNRB: left minimum ramus breadth, RMXRH: right maximum ramus height, RMMBL: right maximum mandibular body length, RMXRB: right maximum ramus breadth, RMNRB: right minimum ramus breadth, RMML: right maximum mandibular length).

**Table 1.** Descriptive statistics of variables and the resulting p-variables of sex differences analysis.

| | All | | M | | F | | |
|---|---|---|---|---|---|---|---|
| Variable | | CI_95 | | CI_95 | | CI_95 | P |
| Age | 73 [60-99] | 71-77 | 76 [65-96] | 73-80 | 75 [65-99] | 73-77 | 0.118≠ |
| BCB | 12.2±0.7 | 12.1-12.3 | 12.5±0.5 | 12.4-12.6 | 11.9±0.6 | 11.7-12.0 | <0.001♯ |
| BANB | 9.0±0.6 | 9.0-9.1 | 9.3±0.6 | 9.2-9.4 | 8.8±0.5 | 8.7-8.9 | <0.001♯ |
| BGP | 9.9±0.6 | 9.9-10.0 | 10.3±0.6 | 10.2-10.4 | 9.6±0.6 | 9.5-9.7 | <0.001♯ |
| RMXRH | 5.7±0.6 | 5.7-5.8 | 6.1±0.5 | 6.0-6.2 | 5.4±0.5 | 5.3-5.5 | <0.001♯ |
| LMMBL | 8.6±0.6 | 8.5-8.6 | 8.8±0.6 | 8.7-8.9 | 8.3±0.5 | 8.2-8.4 | <0.001♯ |
| LMXRB | 3.7±0.4 | 3.6-3.7 | 3.8±0.4 | 3.7-3.9 | 3.5±0.4 | 3.4-3.6 | <0.001♯ |
| LMNRB | 2.7±0.3 | 2.7-2.8 | 2.8±0.3 | 2.8-2.9 | 2.6±0.3 | 2.6-2.7 | <0.001♯ |
| RMML | 3.4±0.1 | 3.4-3.4 | 3.5±0.1 | 3.5-3.5 | 3.4±0.1 | 3.3-3.4 | <0.001♯ |
| LMXRH | 2.3±0.1 | 2.3-2.3 | 2.4±0.1 | 2.4-2.4 | 2.2±0.1 | 2.2-2.3 | <0.001♯ |
| BMFB | 4.5 (2.2-6.1) | 4.5-4.6 | 4.3 (0.5-5.0) | 4.2-4.4 | 4.4 (0.5-6.1) | 4.3-4.5 | <0.001≠ |
| RMMBL | 8.4 (6.2-10.5) | 8.3-8.6 | 8.0 (5.2-9.4) | 7.9-8.1 | 8.2 (5.2-10.5) | 8.0-8.3 | <0.001≠ |
| RMXRB | 4.2 (3-5.2) | 4.1-4.3 | 4.0 (2.6-5.07) | 3.8-4.0 | 4.1 (2.6-5.2) | 4.0-4.1 | <0.001≠ |
| RMNRB | 3.1 (2.0-4.2) | 3.0-3.1 | 2.9 (1.9-4.1) | 2.8-3.0 | 3.0 (1.9-4.2) | 2.9-3.0 | <0.001≠ |
| LMML | 12.6 (9.2-15.0) | 12.3-12.8 | 11.7 (8.3-14.0) | 11.6-11.9 | 12.1 (8.3-15.0) | 11.9-12.2 | <0.001≠ |

** Parametric variables are presented as mean ± standard deviation, and nonparametric variables are presented as median (minimum–maximum). The far-right column shows the p-values of independent t-test and Mann-Whitney U test. Values for males, females and both groups are provided in the table. The 95% confidence intervals for the variables are shown in the table (CI_95). †: The RMML and LMXRH variables did not conform to a normal distribution in their raw form; a square-root transformation was applied and the descriptive values presented for these two variables are therefore expressed on the transformed scale. They are not directly comparable with the raw-scale values of the remaining variables or with the cut-off values reported in Table 2. ≠: p-value from the Mann-Whitney U test. ♯: p-value from the independent t-test. (BCB: bi-condylar breadth, BMFB: bi-mental foramina breadth, BANB: bi-antegonial notch breadth, BGP: bi-gonial breadth, LMXRH: left maximum ramus height, LMMBL: left maximum mandibular body length, LMML: left maximum mandibular length, LMXRB: left maximum ramus breadth, LMNRB: left minimum ramus breadth, RMXRH: right maximum ramus height, RMMBL: right maximum mandibular body length, RMXRB: right maximum ramus breadth, RMNRB: right minimum ramus breadth, RMML: right maximum mandibular length).*

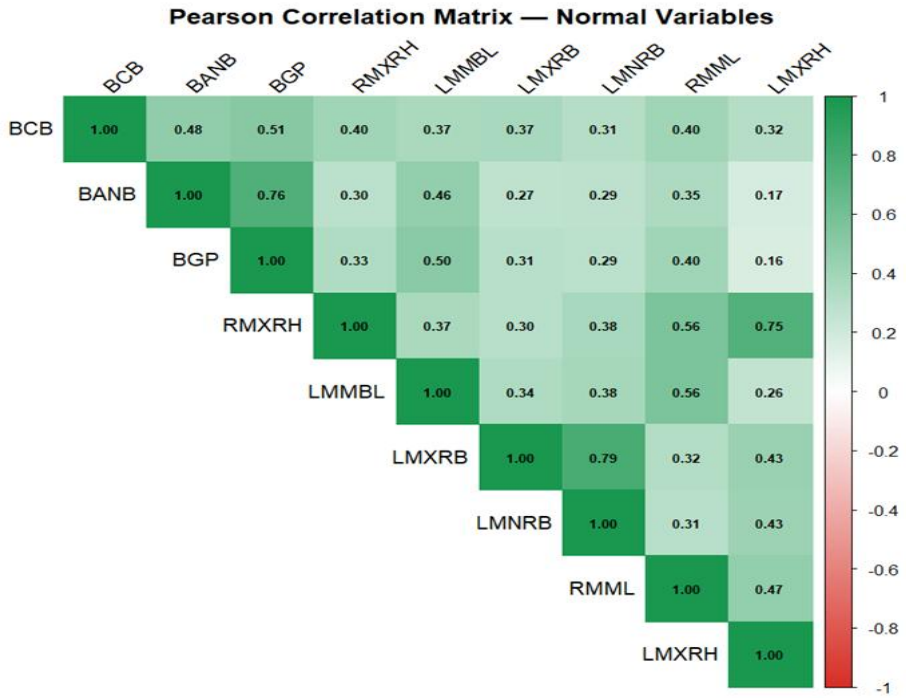


**Figure 9.** Correlation matrix showing the relationship between variables that follow a normal distribution. (BCB: bi-condylar breadth, BMFB: bi-mental foramina breadth, BANB: bi-antegonial notch breadth, BGP: bi-gonial breadth, LMXRH: left maximum ramus height, LMMBL: left maximum mandibular body length, LMML: left maximum mandibular length, LMXRB: left maximum ramus breadth, LMNRB: left minimum ramus breadth, RMXRH: right maximum ramus height, RMMBL: right maximum mandibular body length, RMXRB: right maximum ramus breadth, RMNRB: right minimum ramus breadth, RMML: right maximum mandibular length).

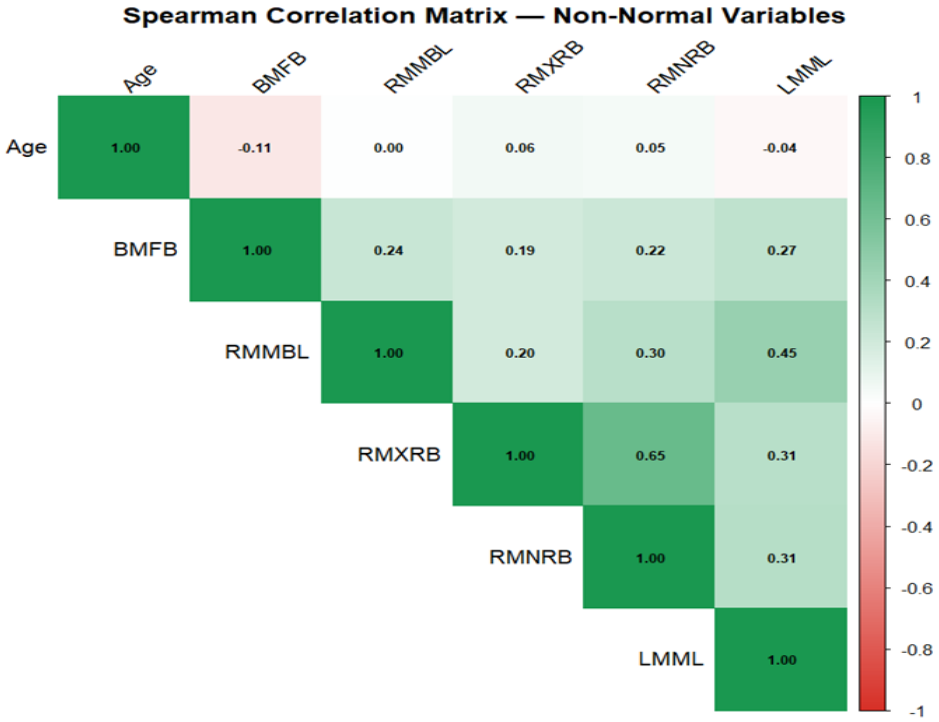


**Figure 10.** Correlation matrix showing the relationship between variables that do not follow a normal distribution. (BCB: bi-condylar breadth, BMFB: bi-mental foramina breadth, BANB: bi-antegonial notch breadth, BGP: bi-gonial breadth, LMXRH: left maximum ramus height, LMMBL: left maximum mandibular body length, LMML: left maximum mandibular length, LMXRB: left maximum ramus breadth, LMNRB: left minimum ramus breadth, RMXRH: right maximum ramus height, RMMBL: right maximum mandibular body length, RMXRB: right maximum ramus breadth, RMNRB: right minimum ramus breadth, RMML: right maximum mandibular length).

correlations were observed, which suggests that the variables are consistent with one another. A strong correlation has been identified especially between the variable pairs LMXRB–LMNRB and RMXRH–LMXRH (Figure 9).

In the correlation analysis conducted for variables that do not follow a normal distribution, the strongest positive relationship was found between the RMXRB and RMNRB variables (rs = .65). This finding indicates that these two variables highly overlap with one another and move in the same direction. A correlation matrix illustrating the relationships between variables that do not follow a normal distribution is shown in Figure 10.

Based on the results of the ROC analysis, the diagnostic performance of the variables was evaluated. The highest diagnostic performance was identified as RMXRH variable among the variables that were evaluated in the study. For this variable, AUC value was calculated as 0.86, cut-off as 5.7, sensitivity as 0.83 and specificity as 0.79. These results indicate that the RMXRH variable provides a good diagnostic discriminatory performance. Overall, it was found that the RMXRH variable had the highest diagnostic accuracy among the variables; the BGP, RMML, and LMXRH variables demonstrated moderate discriminatory performance, while the other variables exhibited limited or weak diagnostic performance (Table 2).

## 4. Discussion

In forensic sciences, identification processes where skeletal structures are used typically begin with determining sex, and the pelvic bone is the preferred choice. However, in cases where the pelvis is missing or otherwise inaccessible, the entire cranium, which exhibits

**Table 2.** The AUC, cutoff, sensitivity, and specificity values from the logistic regression analysis.

| Variable | AUC | Cutoff | Sensitivity | Specificity | Interpretation |
|---|---|---|---|---|---|
| Age | 0.55 | 75.5 | 0.57 | 0.52 | Fail |
| BCB | 0.76 | 12.3 | 0.65 | 0.77 | Fair |
| BMFB | 0.67 | 4.3 | 0.75 | 0.55 | Poor |
| BANB | 0.72 | 9.2 | 0.54 | 0.78 | Fair |
| BGP | 0.79 | 9.8 | 0.84 | 0.64 | Fair |
| RMXRH | 0.86 | 5.7 | 0.83 | 0.79 | Good |
| RMMBL | 0.65 | 8.3 | 0.55 | 0.75 | Poor |
| RMXRB | 0.67 | 4.2 | 0.55 | 0.75 | Poor |
| RMNRB | 0.63 | 3.0 | 0.57 | 0.71 | Poor |
| RMML | 0.79 | 12.2 | 0.66 | 0.85 | Fair |
| LMXRH | 0.79 | 5.6 | 0.71 | 0.77 | Fair |
| LMMBL | 0.70 | 8.8 | 0.47 | 0.87 | Fair |
| LMXRB | 0.67 | 4.0 | 0.40 | 0.86 | Poor |
| LMNRB | 0.66 | 2.8 | 0.60 | 0.68 | Poor |
| LMML | 0.76 | 12.3 | 0.60 | 0.81 | Fair |

**The diagnostic performance of the variables is shown in the Interpretation column. All AUC, cut-off, sensitivity and specificity values were calculated on the raw measurement scale; the cut-off values reported for RMML and LMXRH therefore differ from the square-root transformed descriptive values presented for these two variables in Table 1 (BCB: bi-condylar breadth, BMFB: bi-mental foramina breadth, BANB: bi-antegonial notch breadth, BGP: bi-gonial breadth, LMXRH: left maximum ramus height, LMMBL: left maximum mandibular body length, LMML: left maximum mandibular length, LMXRB: left maximum ramus breadth, LMNRB: left minimum ramus breadth, RMXRH: right maximum ramus height, RMMBL: right maximum mandibular body length, RMXRB: right maximum ramus breadth, RMNRB: right minimum ramus breadth, RMML: right maximum mandibular length).*

a high degree of sexual dimorphism, is used in its place. The present study focuses on the mandible, which is the largest and most compact part of the cranium. In addition, based on the researchers' review of literature, it can be argued that this is the first sex determination study where mandibular parameters are used in both healthy and geriatric population. In line with the literature, the study findings show that the linear mandibular variables reflect a high degree of sexual dimorphism in the geriatric population. The highest linear rate was obtained in the Random Forest algorithm with an Acc value of 93%, while the most significant variable was found to be RMXRH (importance score = 0.1686).

The literature contains numerous studies where sexual dimorphism of the mandible is evaluated through various methods and across different populations. In a retrospective study conducted on the Turkish population and focusing on the metric characteristics of the mandible based on CBCT images, sixteen variables and two software programs were used. The overall accuracy rate of the parameters was determined as 80%; and no significant differences between sexes were found in the statistics for only one variable. While the study concluded that mandibular variables reliably reflect sexual dimorphism, the findings of it were lower than those of the present study [4]. In another study evaluating the role of mandibular anatomical structures in sexual dimorphism in the Turkish population using CBCT images, 16 variables were measured using two different software programs. While the overall accuracy rate was determined to be 80%, the study also emphasised that mandibular features reflect sexual dimorphism in parallel with the current study [14]. In a study aimed to determine sex based on mandibular morphometry using CBCT images in the adult Turkish population, nine of the variables used in the present study were evaluated. It was observed that linear variables measured produced significantly higher results in males similarly with the present study, and a sexual dimorphism rate of 91.5% was reached [14]. In a study designed with the same methodology and objectives in the Eastern Turkey population, 240 participants were assessed with 24 variables. Like the current study, linear parameters were measured at higher values in males, and sexual dimorphism was observed in 97.1% of cases. It is believed that the reason this study achieved a higher rate than the current study is due to the use of a greater number of variables [15]. In a study aiming to determine sex via deep learning models based on the mandibular CT images of Turkish population, 2,310 segmented images were saved in JPEG format. The study found that the hybrid model achieved a 92.5% accuracy rate, which is in consistency with the current study [16]. An anthropometric study investigating the role of mandibular morphological markers in determining sex and age was carried out using 130 dried mandibular bones from the Turkish population. The study concluded that there are significant sex differences in various dimensions of the mandible and that, in general, the males present with larger dimensions than females; and argued that unlike the present study, ramus width did not show a significant difference between the sexes. It is thought that the difference between these two studies is caused by the employment of different methodologies [17]. Another study aimed to determine sex based on only the features of mandibular ramus and was conducted with the CBCT images belonging to the Turkish population. Similarly with the current study, the study findings showed that data pertaining to specifically the

ramus accurately reflected sexual dimorphism rates [18]. In another study aimed to identify the mandibular ramus as a sex marker in Jordanian adults, angular measurements and ratios were calculated using the ImageJ software program. The study findings indicate 80% accuracy in sex determination. It is believed that the lower rate observed in this study is because the study focused solely on the ramus, involved a smaller sample group, and employed a different methodology [19]. In a study examining datasets obtained via CBCT images for sex determination in the Iraqi population through different MLA models, volumetric and linear measurements were made. When statistical results were examined, significant sex differences were found for all variables similarly with the present study, and the highest rate in the MLA was found as 90%, obtained from the GNB model [1]. In a retrospective study focused on mandibular sexual dimorphism in cranial CT images of the South Indian population, higher values in males for all variables were found. In addition, a similar rate of 92.3% sexual dimorphism rate was achieved. It is also noted that the angular measurement accuracy rate is lower compared to the other variables. The absence of angular variables in the current study can be cited as one of its limitations [5]. A study aimed at assessing sex and asymmetry based on the morphometric characteristics of the mandibular condyle via cone-beam computed tomography was conducted on Saudi citizens. As in the present study, while sex differences in the variables were found to be statistically significant, it was concluded that condylar morphometric data alone is insufficient for determining sex [20]. In a sex determination study conducted on the Egyptian population via mandibular measurements from CBCT images, the variables used in the current study were also employed. The findings of the study, as in the present study, highlight that linear measurements are significantly higher in female. While the overall classification accuracy rate was found to be 89.6%, it was also noted that mandibular variables serve as a reliable basis for sex prediction [21]. In a study conducted in Japan where mandibular sexual dimorphism was investigated via CT data, 20 reference points were identified on 3D image models, and mandibular template models were created. The study, which presented an innovative method to the literature, achieved high accuracy rates similarly with the current study [22]. In a study investigating the role of mandibular variables in sex determination conducted with 3D CT images in adults living in Iran, angular and linear variables were employed, similar to those used in the present study. This study emphasised that mandibular variables, the ramus and mandibular length, can be reliably used for sex determination [23]. In a study examining the effect of mandibular size and morphological variables on the accuracy of age and sex determination in the Bulgarian population, geometric morphometric methods were applied to CT images. The findings of the study were in parallel with the current study and revealed significant differences in mandibular dimensions between the sexes [24]. In a study aimed at determining sex via mandibular metric measurements from CBCT images in a Chilean population, it was found that the mandibular ramus was the most sexually dimorphic variable, consistent with the findings of the current study. The study also reported that the mandible displays acceptable sexual dimorphism with an accuracy rate of 87.1% [25]. In a study designed to determine sex based on mandibular variables of the Greek population conducted on three-dimensional CBCT images, volumetric and linear variables

were examined. The study yielded results with an overall accuracy rate of 83.4% and higher accuracy rates were observed in males in line with the findings of the current study [24].

In a study on sex determination where mandibular anthropometric measurements in CBCT images of the Greek population were used in a similar manner with the current study, the differences between the sexes were found to be statistically significant. However, the final model achieved an accuracy rate of 66.7%, which is lower than that of the current study [26]. In a study aimed at analyzing sexual dimorphism observed in the mandibles of the Brazilian population, CBCT images were employed and a 95.1% accuracy rate was achieved. In addition, as in the present study, higher values were observed in males [27]. In a study where mandibular sexual dimorphism was investigated via the CBCT images of adults from the coastal regions of Karnataka and Kerala, higher values were observed in males which highlight mandibular sexual dimorphism. In addition, a detailed analysis of the results between the two regions revealed differences, underscoring the need for sex determination studies to be population specific [26]. In a study on sex determination based on mandibular parameters via cone-beam computed tomography conducted on an Egyptian sample group, the variables of bicondylar distance, mandibular base length, and ramus length displayed significant sexual dimorphism consistently with the findings of the present study [29]. In a study conducted in Indonesia aimed at determining sex from panoramic radiographs through mandibular morphometric analysis, the variables used in the present study were evaluated with Adobe Photoshop® CS6 software. Based on the findings of the study, it was emphasized that the mandible presents sexual dimorphism, and it was argued that the height of the symphysis and the ramus are the most sexually dimorphic parameters [30]. Similarly, the current study also indicates that the most sexually dimorphic variable is the height of ramus. In a study of panoramic radiography where mandibular indices were analyzed for forensic sex determination in South India, the gonial and antegonial angles were measured. The study argued that the antogonal angle can be used to assess the accuracy of sex determination, and have also demonstrated sexual dimorphism in the mandible, as in the present study [31]. In another study where panoramic radiographs were used to investigate sexual dimorphism in mandibular variables of the Saudi Arabian population, higher values were observed in males, consistent with the findings of the present study [32]. In a digital panoramic study conducted in the Sriganganagar population for the same purpose, 200 randomly selected patients were evaluated. The study found that the overall accuracy of the mandible in sex determination was 77.6%, while certain linear parameters were found to have higher values in females. The differences in findings, including lower rates and distinct results compared to the current study may be attributed to the differences in population, imaging method, and age groups [33]. In a study investigating mandibular sexual dimorphism in the Indian population via geometric morphometric methods measured on panoramic images, an overall accuracy of 89.3% was found, similar to the results of the present study [34].

In this study, designed to evaluate the viability of using mandibular parameters for sex prediction in the Maharashtra population, digital orthopantomograms were utilized. The results of the study showed that, apart from the gonial angle, all metric variables were significantly higher in males. The overall

accuracy of the study was found to be 72.5%, which is lower than that of the current study [35]. In another study designed to examine changes in mandibular variables in CT images via geometric morphometric methods and to reflect sexual dimorphism in aging adults, the sample group consisted of individuals aged 40 to 79. Similarly with the current study, the study findings stated that the mandibular sexual dimorphism persists onto the middle and old age [36].

Based on the foundation that temporomandibular joint disorders are more common in females, the muscles obtained from cadavers were examined in a study investigating the relationship between the morphometry of the masticatory muscles and craniofacial dimensions along with the degree of sexual dimorphism. The results of the study revealed significant sex differences in craniofacial dimensions and muscle attachment morphometry, as observed in the present study [37].

***4.1. Conclusions****:* Considering the social and criminal results of it, biological profiling processes is crucial for forensic sciences. Prediction of sex eliminates nearly half of these processes and constitutes a major step. Therefore, the current study was designed to evaluate the variables of the mandible, which is the most durable and compact part of cranium through CT images and to present the sexual dimorphism rate in the geriatric Turkish population via the MLA method. In line with the literature, the results of the study indicate that the mandible can be employed in sex prediction studies and prove that the bone provides high rates of accuracy even in the geriatric period. The researchers believe that the study will contribute to identifying studies of artificial intelligence in the scope of forensic and anthropological sciences.

***Funding:*** *This research did not receive any specific grant from funding agencies in the public, commercial, or not-for-profit sectors.*

***Conflict of Interest:*** *The authors declared no conflict of interest.*

***Ethical Statement:*** *This study was approved by the BAİBÜ Clinical Research Ethics Committee (decision no. 2026/09). As the data were obtained retrospectively from anonymised images held in the BAİBÜ PACS archive, the requirement for written informed consent was waived. All procedures were performed in accordance with the ethical standards of the institutional research committee and with the 1964 Declaration of Helsinki and its later amendments.*

***Acknowledgments:*** *The authors thank the staff of the Radiology Department of Bolu Abant İzzet Baysal University for their assistance with image archiving.*

***Open Access Statement***

*Experimental Biomedical Research is an open access journal and all content is freely available without charge to the user or his/her institution. This journal is licensed under a Creative Commons Attribution 4.0 International License. Users are allowed to read, download, copy, distribute, print, search, or link to the full texts of the articles, or use them for any other lawful purpose, without asking prior permission from the publisher or the author.*

***Copyright (c) 2026:*** *Author (s).*

## References

[1]Baban MTA, Mohammad DN. The accuracy of sex identification using CBCT morphometric measurements of the mandible, with different machine-learning algorithms: a retrospective study. Diagnostics (Basel). 2023;13(14):2342.

[2] Taskın Senol G, Kürtül İ, Ray A, et al. Machine learning algorithms for sex classification by using variables of orbital structures: a computed tomography study. Int J Morphol. 2024;42(4):970-976.

[3] Taskın Senol G, Kürtül İ, Ray A, et al. Sex determination by the machine learning algorithms through using morphometric measurements of the carpal, metacarpal, and phalangeal bones. Int J Morphol. 2023;41(4):1267-1272.

[4] Senol GB, Tuncer MK, Nalcacı N, et al. Role of mandibular anatomical structures in sexual dimorphism in Turkish population: a radiomorphometric CBCT study. J Forensic Odontostomatol. 2022;40(1):53-64.

[5] Lenin V, Das S, V CS, et al. Sex estimation from mandibular morphometry using discriminant analysis: CT scan based retrospective study. Forensic Imaging. 2024;38:200603.

[6] Munhoz L, Okada S, Hisatomi M, et al. Are computed tomography images of the mandible useful in age and sex determination? A forensic science meta-analysis. J Forensic Odontostomatol. 2024;42(1):38-57.

[7] Y. Arifoğlu, Her Yönüyle Anatomi, 4. bs. İstanbul Tıp Kitabevi, 2024.

[8] H. Ozan, Ozan Anatomi, 3. bs. Klinisyen Tıp Kitabevleri, 2014.

[9] Toneva DH, Nikolova SY, Fileva NF, et al. Size and shape of human mandible: sex differences and influence of age on sex estimation accuracy. Leg Med (Tokyo). 2023;65:102322.

[10] Alias A, Ibrahim A, Abu Bakar SN, et al. Anthropometric analysis of mandible: an important step for sex determination. Clin Ter. 2018;169(5):e217-e223.

[11] Olivares JI, Aguilera IA. Validation of the sex estimation method elaborated by Schutkowski in the Granada Osteological Collection of identified infant and young children: analysis of the controversy between the different ways of analysing and interpreting the results. Int J Legal Med. 2016;130(6):1623-1632.

[12] Shaikh SF, Khan S, Shroff G, et al. A comparative study of mandibular ramus dimensions between males and females in cadavers from Maharashtra. Perspect Med Res. 2024;12(2).

[13] Trivunov N, Petrović B, Milutinović S, et al. Sex and age determination of human mandible using anthropological parameters and TCI and Kvaal methods: study of a Serbian medieval sample. Surg Radiol Anat. 2022;44(11):1485-1494.

[14] Çelebi E, Ersoy Kölege SN, Koşkan Ö, Görmez Ö. Evaluation of sex estimation through mandibular morphometric measurements on cone-beam computed tomography images. J Health Sci Med. 2025;8(6):1011-1017.

[15] Mutlu İ, Asirdizer M, Kartal E, et al. Sex estimation from mandible by computerized tomography images and discriminant function analysis in an Eastern Turkish population. East J Med. 2025;30(3):367-381.

[16] Secgin Y, Cakmak M, Senol D, et al. Sex prediction based on computed tomography images of the mandible using deep learning models. Aust J Forensic Sci. 2026.

[17] Tokpınar A, Alkan Y. The role of mandibular morphological markers in determining sex and age: anatomical and anthropometric analysis. Folia Morphol (Warsz). 2024.

[18] Okkesim A, Erhamza TS. Assessment of mandibular ramus for sex determination: retrospective study. J Oral Biol Craniofac Res. 2020;10(4):569-572.

[19] Abualhija D, Revie G, Manica S. Mandibular ramus as a sex predictor in adult Jordanian subjects. Forensic Imaging. 2020;21:200366.

[20] Alam MK, Ganji KK, Munisekhar MS, et al. A 3D cone beam computed tomography (CBCT) investigation of mandibular condyle morphometry: gender determination, disparities, asymmetry assessment and relationship with mandibular size. Saudi Dent J. 2021;33(7):687-692.

[21] Helmy AM, Shalaby N, Aabdallah AY, et al. Evaluation of selected mandibular measurements in sex identification by using cone beam computed tomography in a sample of Egyptian population. Egypt Soc Clin Toxicol J. 2024;12(2).

[22] Suzuki K, Nakano H, Inoue K, et al. Examination of new parameters for sex determination of mandible using Japanese computer tomography data. Dentomaxillofac Radiol. 2020;49(7):20190282.

[23] Ismaili Shahroudi Moqaddam Z, Jamshidi M, Fares F, et al. The diagnostic value of 3-dimensional computerized tomography (3D-CT) scan indicators of mandible bone in sex determination of selected individuals in Tehran. Med J Islam Repub Iran. 2022;36:160.

[24] Christoloukas N, Mitsea A, Kovatsi L, et al. Sex determination based on posterior mandibular measurements using three-dimensional cone-beam computed tomography images. J Imaging Inform Med. 2025.

[25] Ceballos F, Deana NF, Alves N. Sex estimation in a Chilean population by mandibular analysis in cone beam computed tomography images. BMC Oral Health. 2025;25(1):122.

[26] Christoloukas N, Mitsea A, Kovatsi L, et al. Sex determination using linear anthropometric measurements relative to the mandibular reference plane on CBCT 3D images. J Imaging. 2025;11(7):224.

[27] Gamba TO, Alves MC, Haiter-Neto F. Mandibular sexual dimorphism analysis in CBCT scans. J Forensic Leg Med. 2016;38:106-110.

[28] Rao K, Shetty M, Nayak K, et al. Estimation of sexual dimorphism of the mandible in coastal Karnataka and Kerala populations using cone beam computed tomography. J Health Allied Sci NU. 2022;12(2).

[29] Dakhli I, Abu El-Dahab O. Sexual differentiation based on mandibular parameters utilising cone beam computed tomography of a sample of Egyptian population. Int Arch Integr Med. 2020;7(5):24-31.

[30] Kurniawan A, Sosiawan A, Nurrahman TF, et al. Predicting sex from panoramic radiographs using mandibular morphometric analysis in Surabaya, Indonesia. Bull Int Assoc Paleodont. 2023;17(1).

[31] Arthanari A, Sureshbabu S, Ramalingam K, et al. Forensic gender prediction by using mandibular morphometric indices: a panoramic radiograph study. Cureus. 2024;16(3):e56603.

[32] Alanazi Y, Almagdawi EA, Alanazi RB, et al. Morphometric analysis of the mandibular condyle and ramus on panoramic radiographs: a cross-sectional study in Hail, Saudi Arabia. Cureus. 2026;18(1):e101844.

[33] Saloni, Verma P, Mahajan P, et al. Gender determination by morphometric analysis of mandibular ramus in Sriganganagar population: a digital panoramic study. Indian J Dent Res. 2020;31(3):444-448.

[34] Johnson A, Hoggard C, Singh S, et al. Investigating sexual dimorphism of the

human mandible in Indian population using geometric morphometric method. J Indian Acad Forensic Med. 2024;46(4):467-473.

[35] Shirpure P, Mendpara H, Dhenge V. A digital retrospective study: evaluating the reliability of mandibular parameters as sex predictors in the Maharashtra population. J Indian Acad Forensic Med. 2024;46(3):319-324.

[36] Costa Mendes L, Delrieu J, Gillet C, et al. Sexual dimorphism of the mandibular conformational changes in aging human adults: a multislice computed tomographic study by geometric morphometrics. PLoS One. 2021;16(6):e0253564.

[37] She X, Sun S, Damoon BJ, et al. Sexual dimorphisms in three-dimensional masticatory muscle attachment morphometry regulates temporomandibular joint mechanics. J Biomech. 2021;126:110623.